



Models with two Higgs doublets and a light pseudoscalar: A portal to dark matter and the possible $(g - 2)_\mu$ excess

Giorgio Arcadi^{a,*}, Abdelhak Djouadi^{b,c}, Farinaldo da Silva Queiroz^{d,e,f}

^a Dipartimento di Scienze Matematiche e Informatiche, Scienze Fisiche e Scienze della Terra, Università degli Studi di Messina, Via Ferdinando Stagno d'Alcontres 31, I-98166 Messina, Italy

^b CAFPE and Departamento de Física Teórica y del Cosmos, Universidad de Granada, E-18071 Granada, Spain

^c NICPB, Rävåla pst. 10, 10143 Tallinn, Estonia

^d Departamento de Física, Universidade Federal do Rio Grande do Norte, 59078-970, Natal, RN, Brazil

^e International Institute of Physics, Universidade Federal do Rio Grande do Norte, Campus Universitário, Lagoa Nova, Natal-RN 59078-970, Brazil

^f Millennium Institute for Subatomic Physics at High-Energy Frontier (SAPHIR), Fernandez Concha 700, Santiago, Chile

ARTICLE INFO

Article history:

Received 21 January 2022

Received in revised form 3 September 2022

Accepted 5 September 2022

Available online 7 September 2022

Editor: A. Ringwald

ABSTRACT

In the context of a two-Higgs doublet model, supplemented by an additional light pseudoscalar Higgs boson and a stable isosinglet fermion, we consider the possibility of addressing simultaneously the discrepancy from the standard expectation of the anomalous magnetic moment of the muon recently measured at Fermilab and the longstanding problem of the dark matter in the universe which can be accounted for by a thermal weakly interacting massive particle. We show that it is indeed possible, for a range of masses and couplings of the new light pseudoscalar and the fermionic states, to explain at the same time the two features while satisfying all other constraints from astroparticle physics and collider searches, including the constraints from flavor physics.

© 2022 The Author(s). Published by Elsevier B.V. This is an open access article under the CC BY license (<http://creativecommons.org/licenses/by/4.0/>). Funded by SCOAP³.

1. Introduction

A new measurement of the anomalous magnetic moment of the muon, $a_\mu = \frac{1}{2}(g - 2)_\mu$, has been recently released by the Muon $g - 2$ collaboration at Fermilab [1] which, when combined with a previous measurement performed at Brookhaven [2], gives the value [1]

$$a_\mu^{\text{EXP}} = (116592061 \pm 41) \times 10^{-11}, \quad (1)$$

which implies a 4.2σ deviation from the consensus on the Standard Model (SM) contribution [3–24]

$$\Delta a_\mu = a_\mu^{\text{EXP}} - a_\mu^{\text{SM}} = (251 \pm 59) \times 10^{-11}. \quad (2)$$

While not yet exceeding the 5σ target which is needed to claim observation, it is very tempting to attribute this discrepancy to a new phenomenon beyond the ones predicted in the SM, rather to still unknown theoretical or experimental uncertainties. In such a case, the new measurement would probably be the first sign of the so awaited new physics. An explanation of the fact that these possible effects behind this observation have not been observed in

direct searches conducted in the high-energy frontier at the CERN Large Hadron Collider (LHC) [25–27], would be that they are rather due to the presence of light new species which can significantly contribute to the $(g - 2)_\mu$ observable, but are difficult to detect at the LHC as they yield events with small transverse momenta. The new light degrees of freedom could also enter B-meson physics observables (in which some anomalies have also been observed) and in, particular, contribute to the semi-leptonic $b \rightarrow s\mu^+\mu^-$ decay rate, which happens to also be related to muons and slightly deviates from the SM expectation [28].

If all these anomalies are indeed present, it would be theoretically appealing if they are related to the presence of dark matter (DM) in the universe [29]. This DM could appear in the form of a colorless and electrically neutral, weakly interacting massive particle (WIMP) which is stable at cosmological scales [30,31]. Several attempts have been made in this direction, see e.g. Refs. [32–39] for a few examples. In Ref. [34] for instance, a systematic classification of minimal models according to the quantum numbers of their field content [40] has been made and two specific examples of scenarios resolving the $(g - 2)_\mu$ anomaly and with different DM candidates have been proposed: a mixed $SU(2)_L$ singlet-doublet lepton and a real scalar field. In Refs. [36,37], a two Higgs doublet model (2HDM) augmented by an Abelian gauge symmetry and a vector-like fermion family, that contribute to $(g - 2)_\mu$ has also been discussed.

* Corresponding author.

E-mail address: giorgio.arcadi@unime.it (G. Arcadi).

In this note, we propose another solution to the $(g-2)_\mu$ possible discrepancy which also fulfills the requirements for a WIMP DM. It is based on a Higgs sector which is extended to contain two doublets and a light pseudoscalar field a which can serve as a portal to a DM sector, which minimally consists of an SU(2) isosinglet fermion. This 2HD+ a model¹ has recently gained a wide interest as it easily copes with constraints from collider and astroparticle physics [43–47]. Indeed, one can obtain the correct relic density for the DM through its efficient annihilation into SM particles via the s -channel exchange of the a state and, at the same time, evade the stringent XENON1T direct limits in the spin-independent scattering of the DM over nucleons [48], as the DM would not couple to the CP-even Higgs bosons. On the other hand, light pseudoscalar Higgs particles that do not couple strongly to the observed SM-like Higgs boson, can easily evade the LHC bounds from direct Higgs searches [26].

Hence, the pseudoscalar particle present in the model can be rather light and have couplings to isospin-down fermions that are enhanced; it can be thus exchanged between muons and gives a contribution to the $(g-2)_\mu$ [49–56]. Whether this contribution is large enough as to explain the excess observed by the Fermilab experiment, while complying with the set of astrophysical and collider constraints previously mentioned, is the purpose of the present note. We will show that, indeed, there is a range of the masses and couplings of the a boson and the DM fermion that are not excluded by searches at the LHC and elsewhere and by direct and indirect detection experiments, which lead to the correct DM relic abundance and explains the $(g-2)_\mu$ deviation. In addition, the a state would also contribute to the $b \rightarrow sl^+l^-$ process which can be observed in B-meson decays; the decay rate would be particularly enhanced in the case of a light a boson which is emitted on mass shell.

In the next section, we briefly introduce the 2HD+ a model and summarize the theoretical constraints on it. In section 3, we summarize the various experimental constraints from LHC and other collider searches, DM experiments and the contributions to the $(g-2)_\mu$. In section 4, we perform a numerical analysis of the model and delineate the region of parameter space that could explain all observed phenomena. A short conclusion is given in the last section.

2. The 2HD+ a model

The scenario of a two-Higgs doublet model plus a light pseudoscalar state offers the possibility of inducing in a gauge invariant manner, an interaction between a singlet pseudoscalar a boson and the SM fermions. One obtains a coupling of the form $a\bar{f}\gamma_5 f$, via the mixing of a with the pseudoscalar A state of the 2HDM [43–47]. The following potential has been adopted to describe the scalar sector of the model [47]:

$$V = V(\Phi_1, \Phi_2) + \frac{1}{2}m_{a_0}^2 a_0^2 + \frac{\lambda_a}{4}a_0^4 + \left(ik a_0 \Phi_1^\dagger \Phi_2 + \text{h.c.}\right) + \left(\lambda_{1P} a_0^2 \Phi_1^\dagger \Phi_1 + \lambda_{2P} a_0^2 \Phi_2^\dagger \Phi_2\right), \quad (3)$$

where $V(\Phi_1, \Phi_2)$ denotes the potential of the two Higgs doublet fields which can be found in Refs. [57,58]. Notice that CP-conservation in the scalar sector as well as a Z_2 symmetry, to forbid tree level FCNCs, have been assumed. Once the electroweak symmetry is broken, the two doublet fields acquire non-zero expectation values v_1 and v_2 where, as usual, the ratio is denoted

Table 1

Summary of the possible values, in the alignment limit $\beta - \alpha \rightarrow \frac{\pi}{2}$, of the ξ_f parameters describing the couplings of the extra Higgs bosons to the SM fermions.

	Type I	Type II	Lepton-specific (X)	Flipped
ξ_u	$\frac{1}{\tan\beta}$	$\frac{1}{\tan\beta}$	$\frac{1}{\tan\beta}$	$\frac{1}{\tan\beta}$
ξ_d	$-\frac{1}{\tan\beta}$	$\tan\beta$	$-\frac{1}{\tan\beta}$	$\tan\beta$
ξ_l	$-\frac{1}{\tan\beta}$	$\tan\beta$	$\tan\beta$	$-\frac{1}{\tan\beta}$

by $v_1/v_2 = \tan\beta$ with $\sqrt{v_1^2 + v_2^2} = v \simeq 246$ GeV. The scalar sector of the theory will consist of two CP-even h, H states, with h conventionally identified with the 125 GeV boson observed at the LHC, two charged H^\pm bosons and two CP-odd states. The latter are a mixture of the original singlet and 2HDM states a_0 and A_0 obtained from the field rotation

$$\begin{pmatrix} A \\ a \end{pmatrix} = \begin{pmatrix} \cos\theta & \sin\theta \\ -\sin\theta & \cos\theta \end{pmatrix} \begin{pmatrix} A_0 \\ a_0 \end{pmatrix} \quad \text{with} \quad \tan 2\theta = \frac{2\kappa v}{M_A^2 - M_a^2}. \quad (4)$$

In the physical mass basis, the scalar sector of the theory is fully described by the following set of parameters: the physical masses of the five Higgs bosons, $M_h, M_H, M_{H^\pm}, M_a, M_A$, three parameters of the scalar potential, namely $\lambda_{1P}, \lambda_{2P}$ and λ_3 (contained in the 2HDM potential), and finally, the mixing angles entering the quantities $\sin\theta, \tan\beta$ and $\cos(\beta - \alpha)$ with α being the mixing angle among the 2HDM CP-even neutral bosons. It is possible to eliminate the last parameter by imposing the alignment limit, $\beta - \alpha = \pi/2$, which sets the values of the coupling of the lighter h state to fermions and gauge bosons to its corresponding SM values, as favored by the constraints on the 125 GeV Higgs boson properties measurements [25]. In addition, to cope with constraints from high-precision electroweak measurements performed at LEP and elsewhere [59], and in particular to forbid large contributions to the ρ parameter (see however Ref. [60], in view of the recent CDF M_W measurement [61]), we will assume mass degeneracy for the heavier H, A, H^\pm states, $M_H = M_A = M_{H^\pm}$ [62].

The couplings of the physical neutral Higgs bosons to the SM fermions play a crucial role in our context. In the flavor conserving case (for a discussion of the lepton violating case, see e.g. Ref. [63]), they are described by the following Lagrangian

$$\mathcal{L}_{\text{Yuk}} = \sum_f (m_f/v) [g_{hff} h \bar{f} f + g_{Hff} H \bar{f} f - i g_{Aff} A \bar{f} \gamma_5 f - i g_{aff} a \bar{f} \gamma_5 a], \quad (5)$$

where, according to the adopted alignment limit $\alpha = \beta - \pi/2$, one should set the h couplings to their SM values, $g_{hff} = 1$. For the other Higgs couplings, in order to avoid the appearance of flavor-changing neutral currents at tree-level, one assumes the following structure for them (the couplings of the charged Higgs bosons to isospin $\pm \frac{1}{2}$ fermions follow that of the H state)

$$g_{Hff} = \xi_f, \quad g_{Aff} = \cos\theta \xi_f, \quad g_{aff} = -\sin\theta \xi_f, \quad (6)$$

with the parameters ξ_f having four sets of possible assignments, corresponding to four “types” of 2HDM [57] and that are summarized in Table 1.

Among these assignments, only the Type-II and the lepton-specific (also customarily dubbed Type-X) scenarios are of interest for our study, as they feature enhanced couplings of the additional Higgs bosons to the SM charged leptons for large values of $\tan\beta$.

The trilinear interactions between the Higgs states will also have an important impact. In the alignment limit, the pseudoscalar states couple only to the SM-like h boson and an important interaction is the one among the haa states described by the coupling

¹ In fact, this model bears many similarities with a well known benchmark scenario proposed for the next-to-minimal supersymmetric extension of the SM (NMSSM) [41]; see Ref. [42] for a comparison.

$$\lambda_{haa} = \frac{1}{M_h v} \left[\left(M_h^2 + 2M_H^2 - 2M_a^2 - 2\lambda_3 v^2 \right) \sin^2 \theta - 2 \left(\lambda_{p1} \cos^2 \beta + \lambda_{p2} \sin^2 \beta \right) v^2 \cos^2 \theta \right]. \quad (7)$$

There are strong theoretical constraints on the model, in particular conditions on the quartic Higgs couplings in order to have a scalar potential that is bounded from below [64] (similar to the case of a general 2HDM) as well as requirements from perturbative unitarity on the scattering amplitudes of Higgs into gauge boson processes [44]. These constraints have been discussed in e.g. Ref. [42] and we include them in our analysis. In the limit $M_A \gg M_a$ and for a maximal mixing $\sin 2\theta \approx 1$, these induce an upper bound on M_A of about 1.4 TeV which can, however, be weakened by lowering the value of $\sin 2\theta$.

Let us finally introduce and discuss the DM candidate, which will be assumed to be a Dirac fermion (no substantial change of the results is expected in the case of a Majorana fermion) which is isosinglet under the SM gauge group. Because it is not charged under $SU(2)_L$, the DM state has no couplings to gauge bosons and by virtue of the Z_2 symmetry that is introduced in order to make it stable, it couples to Higgs bosons only in pairs. Starting from an initial coupling with the a_0 state, and after electroweak symmetry breaking, the DM will interact with the two pseudoscalar bosons according to the following Lagrangian

$$\mathcal{L}_{\text{DM}} = g_\chi (\cos \theta a + \sin \theta A) \bar{\chi} i \gamma_5 \chi. \quad (8)$$

There are no couplings of the DM fermion to the CP-even Higgs bosons at tree-level and this will have important consequences as we will see in the next section.

3. Implications for collider and astroparticle physics

3.1. Collider constraints and effects in flavor physics

Scenarios like the one under consideration here are, first of all, constrained by high-precision electroweak as well as SM-like Higgs measurements [59,62]. The electroweak constraints can be evaded if all the heavier Higgs states are assumed to be degenerate in mass, i.e. $M_H \simeq M_A \simeq M_{H^\pm} \equiv M$ [65]. The assumption of the alignment limit guarantees, instead, that the lighter h boson is SM-like. As we are interested in situations in which the couplings to isospin $-\frac{1}{2}$ muons are enhanced, only the two 2HDMs of Type II and Type X (lepton-specific) with large values of $\tan \beta$, say $\tan \beta \gtrsim 10$, will be interesting for our analysis.

For what concerns collider constraints, we have first of all the ones coming from searches of the H, A, H^\pm bosons at the LHC. In this regard, the Type-II and Type-X scenarios differ significantly. In the former case, because of the $\tan \beta$ enhancement of the couplings of the neutral Higgs bosons with both down-type quarks and leptons, sizable signals from $pp \rightarrow A/H \rightarrow \tau\tau$ production processes are potentially expected. LHC searches of this signature, see e.g. Ref. [66] for the latest results, have been used to set upper bounds on the value of $\tan \beta$ as function of $M_A = M_H$ in MSSM scenarios such as the hMSSM [67,68] or M_h^{125} [69]. Similar limits could be also adapted to the Type-II 2HD+a model.

There are some notable differences with the previous SUSY scenarios, though. First of all the production cross section of the heavy pseudoscalar A is suppressed, compared to the hMSSM, by a factor $\cos^2 \theta$. As will be seen below, high values of the mixing angles will be considered for our study, hence corresponding to a sizable reduction of the cross section. Furthermore, the decay branching fractions into τ lepton pairs of both H and A bosons are reduced because of the presence of additional decay channels, namely $H \rightarrow aa$, $H \rightarrow aZ$ and $A \rightarrow ha$. For our numerical

study, illustrated in the next subsection, we have recast for the Type-II 2HD+a model, the limits given in Ref. [66] for the hMSSM. Charged Higgs bosons are also actively searched, see e.g. Ref. [70] for a recent account, and exclusion bounds can be imposed on the $[M, \tan \beta]$ parameter plane as well. These constraints tend to affect the very low and very high $\tan \beta$ regions, but in the latter case, searches for the neutral H/A states provide stronger constraints. For our numerical analysis, we will consider the specific parameter values $\tan \beta \lesssim 30$ and $M \geq 1$ TeV, for which all these constraints are evaded.

It was pointed out very recently [71] that LHC can also constrain the mass M_a of the pseudoscalar a via searches of light resonances decaying into muon pairs. We thus include this constraint, adopting the most recent limits given by the CMS [72] and LHCb [73] collaborations. More specifically, for $M_a \lesssim 10$ GeV, we have reexpressed the constraint from LHCb in the $(M_a, \sin \theta)$ variables (the strongest in this mass range) originally formulated for the flipped configuration with $\tan \beta = 0.5$. For larger masses, $M_a \gtrsim 10$ GeV, we have computed the rate $\sigma(pp \rightarrow a) \times \text{BR}(a \rightarrow \mu^+ \mu^-)$ using the programs HIGLU [74] and HDECAY [75,76] and compared the result with the corresponding CMS limit [72].

In addition, the Type-II 2HDM+a possesses peculiar signatures such as mono- h or mono- Z [65,77] final states as well as associated production of the light pseudoscalar state with top or bottom quark pairs [78]. These processes are mostly relevant in the regime $M_a > 2m_\chi$ which does not occur for the benchmarks which will be presented in our numerical analysis.

None of the previously discussed constraints will apply to the lepton specific configuration, since the couplings of the Higgs states to quarks are suppressed for high $\tan \beta$ values. Potentially detectable signals could be nevertheless obtained by looking at the production of the $H/A/H^\pm$ states, which in this case could be light and still comply with the $(g-2)_\mu$ and the lepton universality constraints. The production occurs through purely electroweak processes such as $pp \rightarrow H^\pm A, HH^\pm, HA$ and $H^\pm H^\mp$, that could possibly lead to identifiable signatures such as $3\tau + E_{T,\text{miss}}, 4\tau, 4\tau + W^\pm, 4\tau + Z$ etc. The cross section associated to these signatures is potentially within the reach of the LHC for not too heavy Higgs states. Otherwise, for say $M \gtrsim 300$ GeV, a large data sample such as the one expected at HL-LHC would be required, see for instance Ref. [79]. Nevertheless, dedicated Monte-Carlo analyses would be required for a more precise assessment of the possible exclusion bounds.

In contrast, and until recently (see below), there are less severe bounds on the mass and couplings of the pseudoscalar a and it can be as light as a few GeV and, hence, could explain the $g-2$ anomaly. Searches for a light state with a mass $M_a < M_h$ have been performed in associated a production with $b\bar{b}$ and $\tau^+ \tau^-$ pairs in Z decays at LEP1 [80]. These constrain the abb and $a\tau^+ \tau^-$ couplings to be extremely tiny and smaller than those of the SM-like h boson since $Z \rightarrow b\bar{b}h$ as well as $Z \rightarrow h\tau^+ \tau^-$ topologies with a light h have been unsuccessfully searched for [81]. Also at LEP1, couplings of the a state with gauge bosons through loops of new particles should be severely constrained by searches of the exotic $Z \rightarrow a\gamma$ decay [81]. Additional limits on the Zha coupling come from searches in $e^+ e^- \rightarrow ha$ production at LEP2.

The most severe bound on a light a comes from searches in the $h \rightarrow aa$ and $h \rightarrow Za$ processes [44,46,82] which have been extensively studied. In particular, the decay $h \rightarrow aa$ for $M_a < \frac{1}{2} M_h$ is rather constraining as, for a not too small values of the λ_{haa} coupling in eq. (7), it can have a significant rate, which is given by [43,58]

$$\Gamma(h \rightarrow aa) = \frac{|\lambda_{haa}|^2 M_h}{8\pi} \sqrt{1 - 4M_a^2/M_h^2}. \quad (9)$$

This process has been actively searched for by the ATLAS and CMS collaborations through various topologies, $2b2\mu$, $2b2\tau$, $4b$, $jj\gamma\gamma$, $2\mu2\tau$ and 4τ . Besides, one can apply the general constraint on the invisible width of the SM-like Higgs boson, $\text{BR}(h \rightarrow \text{inv}) < 0.11$ [83], to account for this decay and in this work, we will consider the latter more conservative approach.

To evade this bound, one needs a rather small value of the coupling λ_{haa} , namely $\lesssim \mathcal{O}(10^{-3})$. Such a suppression can be obtained by ad hoc assignments of the parameters $\sin\theta$, λ_{1P} and λ_{2P} , that lead to a cancellation among some contributions in eq. (7). In other words a “blind spot” should occur for the haa coupling. (Note that a similar result could be also obtained in a pure 2HDM; deviation from the alignment limit would be required though [84].) This is the approach that we adopt in our analysis in order to circumvent this constraint.

It is worthwhile asking whether radiative corrections can generate a significant λ_{haa} coupling, despite its fine-tuned suppression at tree-level.² To our knowledge, no detailed computation has been performed for this specific model, contrary to the case of the MSSM for instance; see Ref. [85]. To have an estimate of the corrections to the haa coupling that could be large in our case, namely those due to top and bottom quarks at one-loop, we have substituted into the appropriate MSSM expressions given in Ref. [85], the masses and couplings of the 2HD+a model determined via the Feynrules package [86]. In terms of the Passarino-Veltman loop functions B_0 and C_0 [87], computed using the Package-X [88], we obtain for the relevant triangle diagrams involving the third generation heavy fermions:

$$\lambda_{haa}^{1\text{-loop}} = \frac{1}{16\pi^2} \frac{\sin^2\theta}{v^3 M_h} \sum_{f=\tau,b,t} N_f^c \xi_f^2 m_f^4 \left[2B_0(M_h^2, m_f^2, m_f^2) + (M_h^2 - 2M_a^2) C_0(M_h^2, M_a^2, M_a^2, m_f^2, m_f^2, m_f^2) \right]. \quad (10)$$

where we have regulated the divergent piece of the contribution (that appears in the two-point function B_0) in the $\overline{\text{MS}}$ scheme by subtracting the pole which, in a full calculation, should be canceled by the corresponding one of the counterterm of the bare λ_{haa} coupling.

Given the dependence on the fourth power of the mass of the fermion running in the loop, eq. (10) is essentially determined by the contribution from the top quark and, for high $\tan\beta$ values, from the b -quark and τ -lepton. An evaluation of eq. (10) considering the ranges $10\text{GeV} < M_a < 20\text{GeV}$, $0.5 < \sin\theta < 0.7$ and $30 < \tan\beta < 50$, relevant for the $g-2$ (see below), we obtain a variation in the range $\lambda_{haa}^{1\text{-loop}} = 10^{-3} - 10^{-4}$ in the Type-II 2HD+a case. This leads to a branching ratio for the $h \rightarrow aa$ decay that is well below the requested limit.

Let us finally turn to constraints from flavor physics. Such a light particle could affect a broad variety of low energy processes, in particular if it has enhanced couplings to the isospin down-type fermions. For instance, the emission of a light a modifies the decay rates of B and K mesons [89] in Type II models. For the region of interest in the light of the $g-2$ anomaly, the most relevant

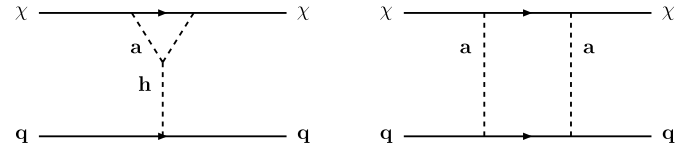


Fig. 1. Generic Feynman diagrams responsible for the loop induced scattering of the DM state on quarks in the two Higgs doublet plus a light pseudoscalar model.

processes are the decays $\Upsilon \rightarrow a\gamma$, $B_s \rightarrow \mu^+\mu^-$ and $B \rightarrow K\mu^+\mu^-$. The experimental bounds on these processes have been translated into constraints for the 2HD+a scenario in Ref. [90] and will be adopted as well for the present study.

In particular, the $B_s \rightarrow \mu^+\mu^-$ decay should receive potentially large contributions from the a state if it is light and has large couplings b -quarks and muons. In the case of the lepton specific configuration, comparatively strong bounds as in the Type-II case can be derived by considering the searches of light leptophilic bosons recently performed by the BaBar collaboration [91]. A further strong constraint comes from violation of lepton universality in the decays of the Z boson and the τ lepton. We have adapted to the present 2HD+a model, all the constraints determined for the 2HDM in Refs. [84,92]. We finally mention the lower bound from the decay $b \rightarrow s\gamma$ on the H^\pm mass (and hence also on M_A and M_H) for the Type-II model, $M_{H^\pm} > 570\text{GeV}$ [93].

3.2. Dark matter constraints and requirements

The 2HD+light a model, as a gauge invariant embedding of a pseudoscalar portal for a SM singlet DM, presents remarkable differences with respect to the other scenarios of fermionic DM connected to the Higgs sector. First, the absence of a coupling between the DM and the CP-even 2HDM states forbids spin-independent interactions for the DM at tree level. These interactions are crucial for direct detection and arise only at the one-loop level. Some Feynman diagrams which contribute to the elastic scattering of the DM with nucleons at this level are shown in Fig. 1. For simplicity, we have depicted only the contribution with a boson exchange but all possible combinations of exchanges of the a , A states should be included, although the contributions with A exchange will be far smaller.

To compute the scattering cross section of the DM over protons, which is needed to be compared with the experimental bounds, we relied on the most recent computations performed in Refs. [94,95] (see also Ref. [90,96] for earlier estimates). The elastic DM cross section determined in this way, has been compared with the most stringent experimental constraints as given by the XENON1T experiment [48].

For what concerns the DM cosmological relic density, we will assume the conventional freeze-out paradigm in which the experimentally favored value $\Omega_\chi h^2 \approx 0.12$ [29] is achieved via the appropriate annihilation of the DM states into SM particles. Throughout the present work, we will assume a relatively light DM particle, with a mass $m_\chi < m_t < M$. Under such a hypothesis, the DM relic density will be mostly accounted for by annihilation into $\tau^+\tau^-$ and $b\bar{b}$ final states for Type II 2HDMs and only $\tau^+\tau^-$ in the lepton-specific or Type X model. The channels with ha , Za and aa final states should also be included in the annihilation subprocesses when they are kinematically accessible. Approximate expressions of the rates of these annihilation channels can be found, for example, in Ref. [42].

Given the fact that the DM annihilation rate into SM fermion final states is s -wave dominated, the model is also sensitive to constraints from DM indirect detection. We have thus included in our study the limits imposed by searches of γ -ray continuous lines as determined by the FERMI-LAT collaboration [97,98] and trans-

² In fact, since we are not specifying the region of parameter space in which it should occur, one could ask for a very small or vanishing $h \rightarrow aa$ decay rate at the renormalized level, i.e. when including radiative corrections. We will nevertheless attempt in the following to estimate the size of the one-loop corrections from the diagrams which are relevant to our discussion here, namely, large bottom-quark Yukawa couplings that occur at high $\tan\beta$. The full calculation, including also the diagrams involving the trilinear and quadrilinear scalar couplings (which should be small if one assumes small couplings and large 2HDM Higgs masses as it is assumed here) is beyond the scope of this letter and will be given in a forthcoming publication.

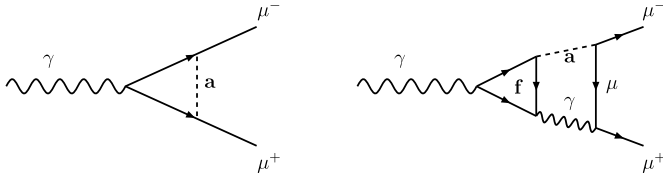


Fig. 2. Generic Feynman diagrams responsible for the one-loop (left) and two-loop (right) contributions of a neutral pseudoscalar Higgs boson to the $(g-2)_\mu$.

lated them into upper limits on the annihilation cross sections into $\tau^+\tau^-$ and $\bar{b}b$ final states.

3.3. Contributions to the $g-2$

Generic neutral Higgs bosons Φ contribute to the muon $g-2$ first at the one-loop level when they are exchanged between the two muon legs³ in the $\gamma\mu^+\mu^-$ vertex, Fig. 2 (left). They give rise to contributions that are proportional to $m_\mu^4/M_\Phi^2 \times g_{\Phi\mu\mu}^2$ where one power of m_μ comes from the definition, one from the kinematics and two powers come from the Yukawa couplings. When the latter are enhanced, $g_{\Phi\mu\mu} \gg 1$, the impact can be sizeable but only if the mass of the exchanged Higgs state is not too large, $M_\Phi \ll 100$ GeV. In view of the severe bounds on the 2HDM Higgs particles from direct and indirect collider searches [62], the only state that can generate a significant contribution is the pseudoscalar a boson. This occurs when it has *i*) a mass below the 10 GeV range, *ii*) enhanced Yukawa couplings, meaning fermionic couplings of Type II and X with large $\tan\beta$ values, and *iii*) a significant mixing with the A boson, $\sin\theta = \mathcal{O}(1)$. In the limit $M_a \gg m_\mu$, one obtains at one-loop [49] (see also Ref. [50])

$$\delta a_\mu^{1\text{-loop}} \approx -\frac{\alpha}{8\pi \sin^2\theta_W} \frac{m_\mu^4}{M_W^2 M_a^2} g_{a\mu\mu}^2 \left[\log\left(\frac{M_a^2}{m_\mu^2}\right) - \frac{11}{6} \right]. \quad (11)$$

Hence, in absolute value, one can indeed generate an adequate contribution to $|a_\mu|$ for a masses below a few 10 GeV and $\tan\beta$ values above 20. However, because the logarithm is large and positive, the one-loop contribution of the a state is in fact always negative and thus, cannot explain the (positive) excess observed by the Fermilab experiment, eq. (2).

Nevertheless, there are also possible contributions to δa_μ which come from some particular Barr-Zee type diagrams [99] occurring at the two-loop level [51–53] and which can be important. Indeed, as shown in the right-hand diagram of Fig. 2, one can generate a heavy fermion loop, $f = t, b, \tau$, that couple to the primary photon, in which a Higgs and a photon can be emitted before ending with the final muon lines.⁴ Although suppressed by two powers of the electroweak coupling, the contribution is enhanced by a factor m_f^2/m_μ^2 relative to the one-loop diagram. The a contribution at this level, in terms of the coupling g_{aff} , color number N_c^f and electric charge Q_f of the loop fermion f with mass m_f , reads [51–53]

$$\delta a_\mu^{2\text{-loop}} = \frac{\alpha^2}{8\pi^2 \sin^2\theta_W} \frac{m_\mu^2}{M_W^2} g_{a\mu\mu} \sum_f g_{aff} N_c^f Q_f \frac{m_f^2}{M_a^2} F\left(\frac{m_f^2}{M_a^2}\right), \quad (12)$$

with the function F defined by

$$F(r) = \int_0^1 dx \frac{\log(r) - \log[x(1-x)]}{r - x(1-x)}. \quad (13)$$

This contribution turns out to be larger than the one-loop contribution and with the correct positive sign that allows to explain the discrepancy of the measurement from the standard value. Again, this occurs for a masses of a few GeV and moderately large $\tan\beta$ values which make that only closed loops of the bottom quark and the tau lepton, which also have couplings $g_{aff} \propto \tan\beta$ in Type II and Type X scenarios, generate substantial contributions.

4. Numerical analysis

We are now ready to present our numerical analysis, taking into account all the ingredients that were presented in the previous sections. They are summarized in Fig. 3 to Fig. 5. The first and last figures show the summary of the constraints in the $[M_a, \tan\beta]$ plane for two benchmark scenarios in, respectively, the Type-II and Type X (lepton specific) configurations for the Higgs-fermion couplings. In each figure, we have considered two values of the DM mass, namely $m_\chi = 60$ GeV and $m_\chi = 150$ GeV, and the values of the coupling g_χ and of $\sin\theta$ were chosen in such a way that the correct DM relic density and a viable fit of $(g-2)_\mu$ could be simultaneously achieved. In all cases we have taken $\sin\theta \gtrsim 0.5$, while the 2HDM H, A and H^\pm states are assumed to have a common mass of $M = 1$ TeV in Type II and $M = 300$ GeV in Type X scenarios. The DM constraints, namely from direct detection from XENON1T and indirect detection from FERMI, as well as flavor constraints have also been included.

As it should be evident from the figures, in Type-II and Type X scenarios, there is indeed an overlap between the regions corresponding to the correct relic density for the DM state (in dark gray in each panel) and the regions reproducing the $(g-2)_\mu$ anomaly within 1σ (green bands) and 2σ (yellow bands). However, these regions differ as for the considered ranges of $\tan\beta$ values. In the former case, because of the $\tan\beta$ enhancement of the Yukawa coupling of the bottom quarks, we had to impose the limit $\tan\beta \leq 60$ from the requirement of a perturbative coupling. Such a constraint is not present in the lepton-specific Type X model and, hence, higher values of $\tan\beta$ can be allowed. This feature influences strongly the allowed regions favored by the $(g-2)_\mu$ value which, indeed, tends to favor the lepton-specific scenario. In all cases, we need a sizable value of the mixing angle θ , in other words require a significant doublet-like component for the pseudoscalar a boson.

Besides this aspect, the Type-II and Type X models differ from the set of complementary constraints which are applied, besides the ones from the $(g-2)_\mu$ and the relic density Ωh^2 . Indeed, in the former case with enhanced g_{abb} couplings, one observes that the mass range $M_a \lesssim 5$ GeV is almost entirely excluded by the bounds from $B \rightarrow K\mu\mu$ and $\Upsilon \rightarrow \gamma a$ decays (we have labeled the ensemble of the two bounds - depicted by the hatched areas in red - as “LHCb” in the plots). Fig. 3 also shows in hatched red, the regions in which the rate of $B_s \rightarrow \mu^+\mu^-$ exceeds the experimental determination [28] by more than 2σ .

For the DM constraints, the regions of parameter space excluded by direct and indirect detection experiments are shown, respectively, as hatched areas in blue and cyan. Note that indirect detection bounds appear only for $m_\chi = 60$ GeV since current

³ For charged Higgs bosons, there is an additional one-loop diagram in which the photon couples to the charged Higgses and a ν_μ neutrino is exchanged between the two muons.

⁴ There is also the possibility of exchanging a Z boson instead of the internal photon but the corresponding contribution is two orders of magnitude smaller and can be thus ignored.

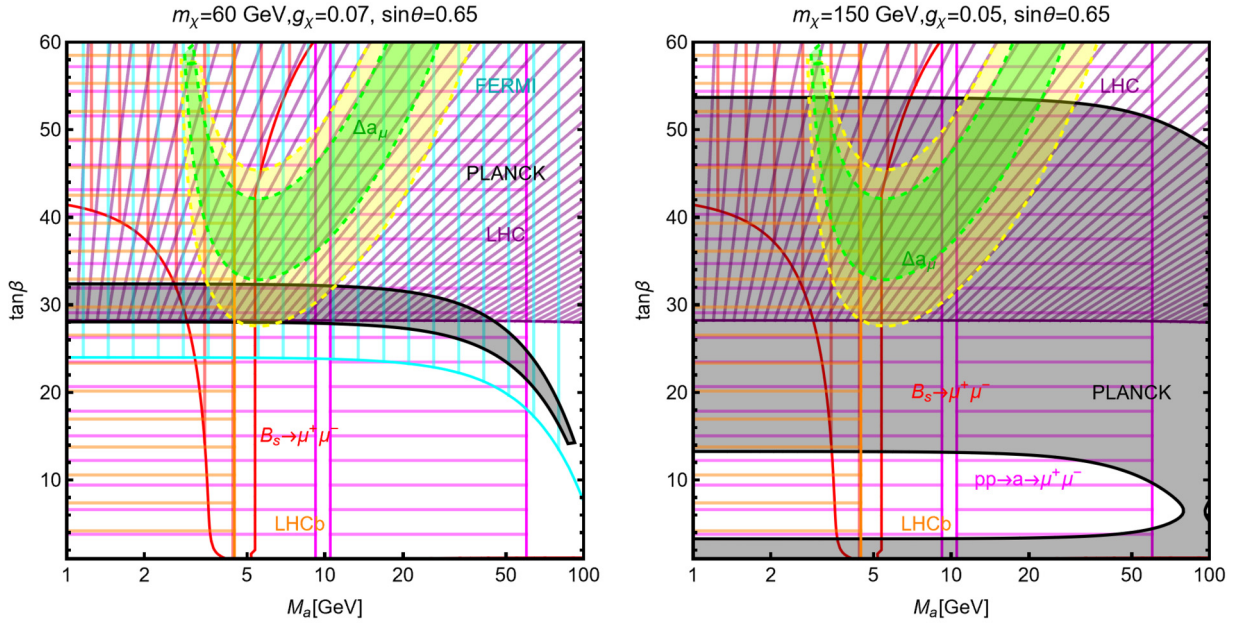


Fig. 3. The summary of constraints, in the $[M_a, \tan\beta]$ plane for the Type-II 2HDM+a state for two choices of the $(m_\chi, g_\chi, \sin\theta)$ parameter set, reported on top the corresponding panels. In each plot, the colored black bands correspond to the correct DM relic density, the green (yellow) band corresponds to a viable fit of the $(g-2)_\mu$ anomaly within $1(2)\sigma$. The red regions correspond to a rate for the $B_s \rightarrow \mu^+\mu^-$ process exceeding the experimental determination. The blue and hatched regions correspond to the exclusion from direct DM searches by XENON1T and indirect DM searches from FERMI-LAT, while the orange region is excluded by constraints from low energy processes. Finally, the purple and magenta hatched regions are excluded, respectively by LHC searches of H/A bosons decaying into $\tau\bar{\tau}$ and a bosons decaying into $\mu\bar{\mu}$. For definiteness we have set the 2HDM mass scale M to 1 TeV.

experiments have not yet reached enough sensitivity to probe the freeze-out paradigm for high DM masses.

Most important, the Type-II scenario is potentially subject to strong LHC constraints. First of all one has to consider searches of resonances decaying into τ pairs which exclude the region highlighted in hatched purple. As can be seen, one has the upper bound $\tan\beta \lesssim 28$, weaker than the corresponding limit in the hMSSM, namely $\tan\beta \lesssim 10$, but still excluding most of the region fitting the $(g-2)_\mu$ anomaly, except for a small portion of the 2σ region.

Nevertheless, as pointed out recently [71], an even stronger bound comes from searches of light resonances produced in gluon or b -quark fusion and decaying into $\mu^+\mu^-$ [72,73]. This bound is particularly effective in the Type-II model since all the couplings involved in a production and decay are $\tan\beta$ enhanced. The excluded region is shown in hatched magenta in Fig. 3 and, as it can be seen, it contains the whole region fitting the $(g-2)_\mu$ anomaly with the exception of a tiny strip around $M_a \simeq 10$ GeV.

To be more explicit, Fig. 4 shows the evolution of the LHC bounds with the model parameters. The left panel shows in magenta (purple) the excluded region by searches of the $pp \rightarrow H/A \rightarrow \tau^+\tau^-$ process in the $[M, \tan\beta]$ for $\sin\theta = 0.5(0.7)$. The regions enclosed between the magenta/purple dashed lines correspond to a viable fit, i.e. within 2σ , of the $(g-2)_\mu$ anomaly. For sake of comparison, we also show the excluded region in the case of the hMSSM. Nevertheless, the tension between the LHC bounds from searches of heavy resonances and the $(g-2)_\mu$ excess interpretation can be relaxed by increasing the value of M . Indeed, while the extension in the $[M_a, \tan\beta]$ plane of the region accounting for the $(g-2)_\mu$ excess is affected very little for higher M , the LHC constraint is progressively relaxed. For instance, we find that the upper bound on $\tan\beta$ moves to $\tan\beta \lesssim 35(48)$ for $M = 1.2(1.4)$ TeV.

Very different is the situation in the case of light resonance searches. The right panel of Fig. 4 shows the excluded region in the $[M_a, \sin\theta]$ plane for $\tan\beta = 40$ and $M = 1.2$ TeV. This region is compared with the $1\sigma(2\sigma)$ $(g-2)_\mu$ band shown in green

(yellow). In agreement with the findings shown in Fig. 3, the limit from $pp \rightarrow a \rightarrow \mu^+\mu^-$ searches strongly disfavor the Type II 2HD+a as an interpretation of the $g-2$ anomaly. The model is however not definitely ruled-out as there is still a small range of M_a values evading the constraint.

Moving to the case of the lepton specific 2HD+a case, for which the constraints are shown in Fig. 5, we notice again that the region $M_a \lesssim 5$ GeV is excluded by searches of new light states. A comparatively stronger bound, with respect to the Type-II scenario, comes from $B_s \rightarrow \mu^+\mu^-$. This is due to the choice $M = 300$ GeV which implies a sizable contribution to the rate of this process also from Higgs bosons other than a . The choice of this low mass scale is needed to comply with bounds from violation of lepton universality in Z and τ decays which are severe. A stronger hierarchy between M_a and M would have completely ruled out the region corresponding to the fit of the $(g-2)_\mu$ measurement; see also Ref. [92].

No exclusion from direct detection experiments appears. This is due to the fact that the $1/\tan\beta$ dependence of the a/A couplings to quarks causes a suppression of the contribution from the box diagram in Fig. 1, while the contribution of the triangle diagram, usually dominated by the exchange of the light pseudoscalar a state, is suppressed by the requirement $\lambda_{haa} \simeq 0$ to avoid a too large rate for the exotic decay of the SM-like Higgs boson into a pairs. As can be seen, the region accounting for the $(g-2)_\mu$ excess is tightly constrained. Nevertheless, a combined fit of $(g-2)_\mu$ and the correct relic density is still possible in the $M_a \simeq 10-20$ GeV range, for the DM mass value $m_\chi = 150$ GeV. The lighter DM benchmark is, instead, again disfavored by DM indirect detection as shown in the left panel of Fig. 5.

As already mentioned before, the 2HD+a Type-X benchmarks that we illustrate in Fig. 5 easily evade the LHC bounds that are severe in the Type II scenario. To further strengthen this point, we confront in Fig. 6 the theoretical expectations for the cross-sections of heavy A production in the process $pp \rightarrow A \rightarrow \tau^+\tau^-$ and light a production in the process $pp \rightarrow a \rightarrow \mu^+\mu^-$ as functions of the relevant Higgs mass and for the values $\tan\beta = 20, 50, 80$. The cross-

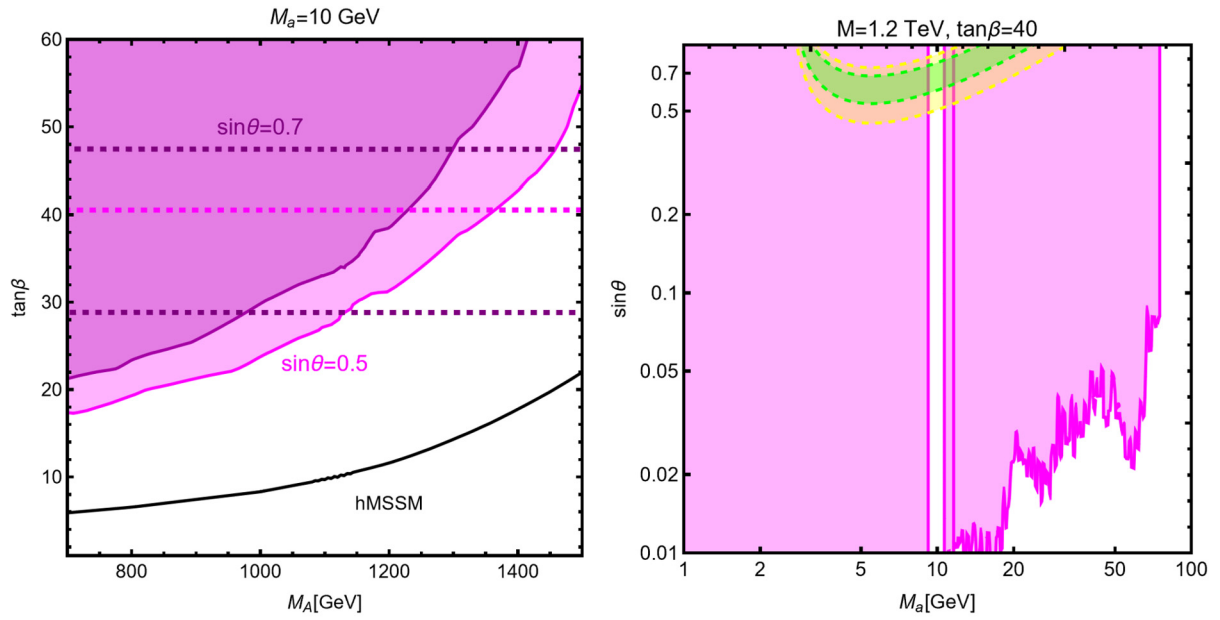


Fig. 4. Most relevant LHC constraints on the 2HD+a Type II. The left panel shows in magenta (purple) the excluded regions by searches of heavy resonances decaying into $\tau^+\tau^-$ in the $[M, \tan\beta]$ plane for $M_a = 10$ GeV and $\sin\theta = 0.5$ (0.7). The regions between the dashed lines, correspond to a viable fit within 2σ of the $(g-2)_\mu$ anomaly. For reference, the exclusion line for the hMSSM is shown as well. The right panel shows the exclusion from searches of light resonances in the $[M_a, \sin\theta]$ plane for $M = 1.2$ TeV and $\tan\beta = 40$. The green (yellow) band corresponds to a fit of $g-2$ at $1(2)\sigma$.

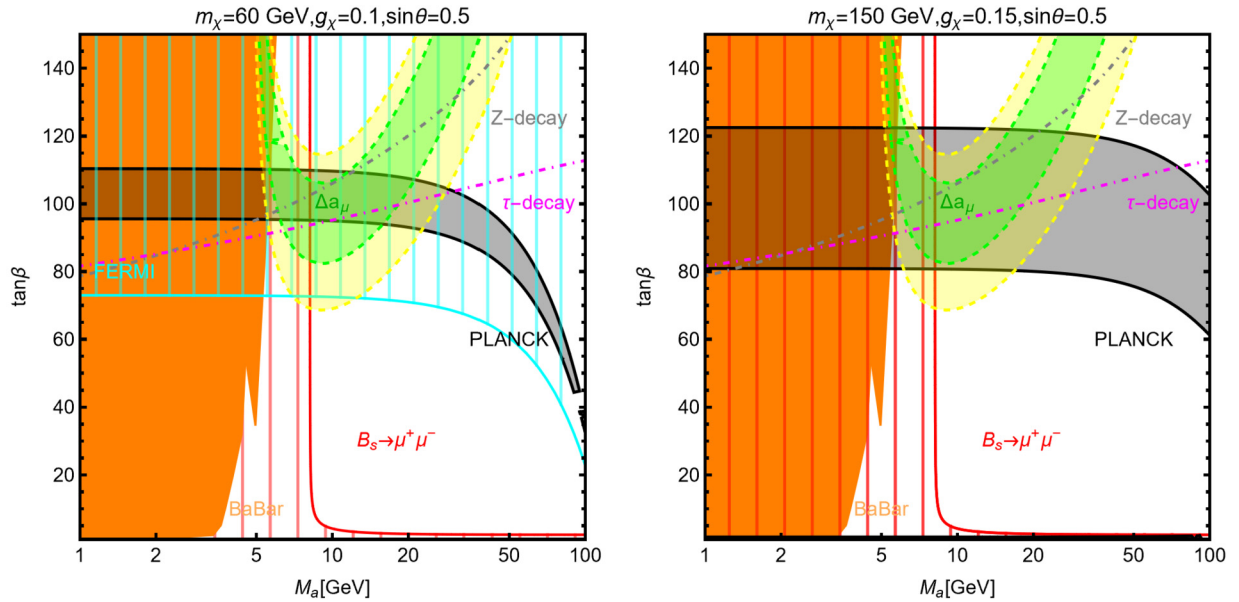


Fig. 5. The same as in Fig. 3 but for the lepton-specific Type X 2HD+a scenario with a 2HDM mass scale set to $M = 300$ GeV. Here, we have included bounds from Z-boson and τ -lepton decays which exclude the regions above the dot-dashed gray and magenta lines.

sections at the $\sqrt{s} = 13$ TeV LHC, which have been determined using the SusHi package [100] as in the previously discussed case, are confronted to the exclusion experimental bounds (represented as black solid lines) that were derived in, respectively, Ref. [66] and Ref. [72]. As can be seen, the LHC constraints are thus not a problem in the Type-X case.

5. Conclusions

In this note, we have studied a beyond the SM scenario in which the Higgs sector is enlarged to contain two doublets of scalar fields as well as an additional pseudoscalar Higgs boson, while the matter sector is extended by an additional electroweak isosinglet fermion which is made stable by imposing a discrete

symmetry. The singlet pseudoscalar state should be rather light and substantially mix with the heavier one of the 2HDM. One can arrange that it has strongly enhanced Yukawa couplings to isospin down-type fermions such as the muons (and eventually bottom quarks) in the Type II and Type X 2HDM scenarios, by choosing the ratio of vacuum expectation values of the two doublet fields to be rather large, $\tan\beta \gg 1$.

Such a scenario also copes with constraints from flavor physics and, for instance, provides the correct rate for the decay $B_s \rightarrow \mu^+\mu^-$. Cosmological and astrophysical requirements on the additional DM fermion, namely that it leads to the correct cosmological DM abundance and evades the limits from direct and indirect DM detection, can be also fulfilled. Finally, we have shown that for masses and couplings that are allowed by the previous constraints

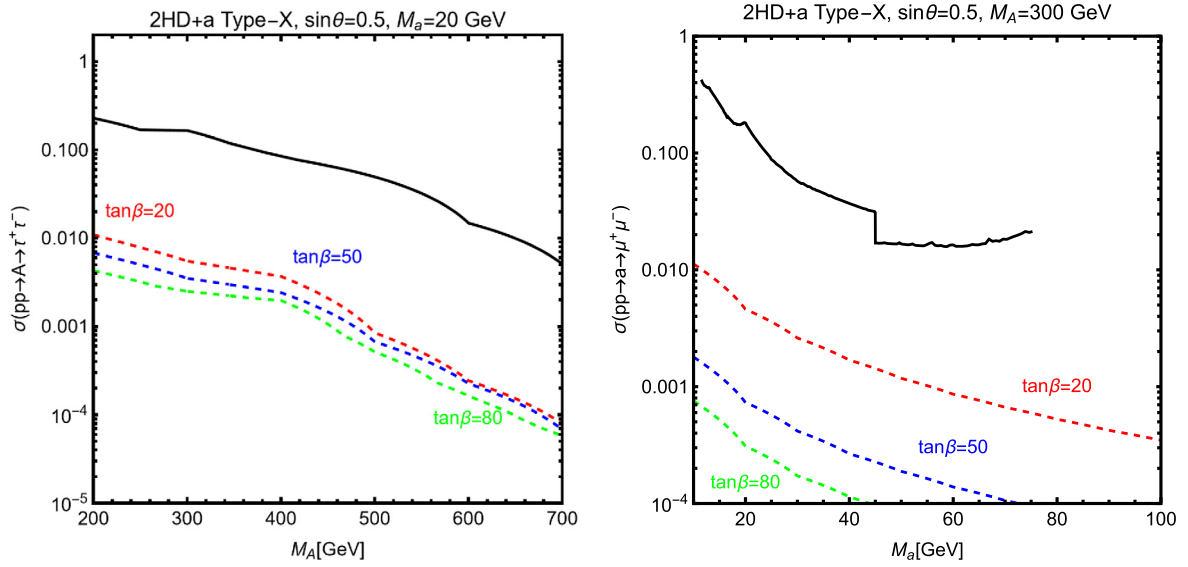


Fig. 6. *Left:* the theoretical predictions for the cross section of the process $pp \rightarrow A \rightarrow \tau^+\tau^-$, at the LHC as a function of M_A , for three values of $\tan\beta$, namely 20 (dashed red), 50 (dashed blue) and 80 (dashed green) and with the assignments of the other relevant parameters as reported on top of the panel; the black line represents the experimental limit. *Right:* the theoretical prediction for the cross-section of the process $pp \rightarrow a \rightarrow \mu^+\mu^-$ as function of M_a ; the color code is the same as in the left panel. The black curve representing the experimental sensitivity stops at around 75 GeV since the search presented in [72] is not sensitive in the 75–110 GeV mass range.

and requirements, one can arrange such that the pseudoscalar a state contributes to the muon $(g-2)$ and explains the 4.2σ deviation of the value recently measured at Fermilab from the one expected in the SM. Nevertheless, one of the two considered scenarios, namely Type II, is challenged by LHC searches of resonances decaying into lepton pairs, if not totally excluded. A definite assessment of the area of parameter space in which this model might be still viable requires a dedicated analysis (which includes some of the experimental aspects) and is postponed to a future publication. The Type X scenario is not affected by this constraint.

In any case, if the anomaly in the measurement of the $(g-2)_\mu$ persists and is magnified by future more precise measurements, the 2HD+a scenario could be one of the most interesting viable solutions to resolve the discrepancy as it would also address the DM issue which is very important in particle physics and cosmology. In this case, more dedicated searches for such additional Higgs and DM states should be made and these would benefit from the next run and high-luminosity option of the LHC and the increase in sensitivity of various astroparticle experiments that are planned in the near future.

Declaration of competing interest

The authors declare that they have no known competing financial interests or personal relationships that could have appeared to influence the work reported in this paper.

Data availability

No data was used for the research described in the article.

Acknowledgements

AD is supported by the Estonian Research Council (ERC) grant MOBTT86 and by the Junta de Andalucía through the Talentia Senior program as well as by A-FQM-211-UGR18, P18-FR-4314 with ERDF. FSQ have been supported by the São Paulo Research Foundation (FAPESP) through Grant No. 2015/15897-1 and ICTP-SAIFR FAPESP grant 2016/01343-7. FSQ work was supported by the Serapilheira Institute (grant number Serra-1912-31613), ANID – Mil-

lennium Program – ICN2019-044, and CNPq grants 303817/2018-6 and 421952/2018-0.

References

- [1] B. Abi, et al., Measurement of the positive muon anomalous magnetic moment to 0.46 ppm, *Phys. Rev. Lett.* 126 (4 2021) 141801.
- [2] G.W. Bennett, et al., Final report of the muon E821 anomalous magnetic moment measurement at BNL, *Phys. Rev. D* 73 (2006) 072003.
- [3] T. Aoyama, et al., The anomalous magnetic moment of the muon in the Standard Model, *Phys. Rep.* 887 (2020) 1–166.
- [4] Tatsumi Aoyama, Masashi Hayakawa, Toichiro Kinoshita, Makiko Nio, Complete tenth-order QED contribution to the muon $g-2$, *Phys. Rev. Lett.* 109 (2012) 111808.
- [5] Tatsumi Aoyama, Toichiro Kinoshita, Makiko Nio, Theory of the anomalous magnetic moment of the electron, *Atoms* 7 (1) (2019) 28.
- [6] Andrzej Czarnecki, William J. Marciano, Arkady Vainshtein, Refinements in electroweak contributions to the muon anomalous magnetic moment, *Phys. Rev. D* 67 (2003) 073006, Erratum: *Phys. Rev. D* 73 (2006) 119901.
- [7] C. Gnendiger, D. Stöckinger, H. Stöckinger-Kim, The electroweak contributions to $(g-2)_\mu$ after the Higgs boson mass measurement, *Phys. Rev. D* 88 (2013) 053005.
- [8] M. Davier, A. Hoecker, B. Malaescu, Z. Zhang, Reevaluation of the hadronic vacuum polarization contributions to the Standard Model predictions of the muon $g-2$ and $\alpha(m_Z^2)$ using newest hadronic cross-section data, *Eur. Phys. J. C* 77 (12) (2017) 827.
- [9] Alexander Keshavarzi, Daisuke Nomura, Thomas Teubner, Muon $g-2$ and $\alpha(M_Z^2)$: a new data-based analysis, *Phys. Rev. D* 97 (11) (2018) 114025.
- [10] Gilberto Colangelo, Martin Hoferichter, Peter Stoffer, Two-pion contribution to hadronic vacuum polarization, *J. High Energy Phys.* 02 (2019) 006.
- [11] Martin Hoferichter, Bai-Long Hoid, Bastian Kubis, Three-pion contribution to hadronic vacuum polarization, *J. High Energy Phys.* 08 (2019) 137.
- [12] M. Davier, A. Hoecker, B. Malaescu, Z. Zhang, A new evaluation of the hadronic vacuum polarization contributions to the muon anomalous magnetic moment and to $\alpha(m_Z^2)$, *Eur. Phys. J. C* 80 (3) (2020) 241, Erratum: *Eur. Phys. J. C* 80 (2020) 410.
- [13] Alexander Keshavarzi, Daisuke Nomura, Thomas Teubner, $g-2$ of charged leptons, $\alpha(M_Z^2)$, and the hyperfine splitting of muonium, *Phys. Rev. D* 101 (1) (2020) 014029.
- [14] A. Kurz, T. Liu, P. Marquard, M. Steinhauser, Hadronic contribution to the muon anomalous magnetic moment to NNLO, *Phys. Lett. B* 734 (2014) 144–147.
- [15] Kirill Melnikov, Arkady Vainshtein, Hadronic light-by-light scattering contribution to the muon anomalous magnetic moment revisited, *Phys. Rev. D* 70 (2004) 113006.
- [16] Pere Masjuan, Pablo Sanchez-Puertas, Pseudoscalar-pole contribution to the $(g_\mu-2)$: a rational approach, *Phys. Rev. D* 95 (5) (2017) 054026.

- [17] G. Colangelo, M. Hoferichter, M. Procura, P. Stoffer, Dispersion relation for hadronic light-by-light scattering: two-pion contributions, *J. High Energy Phys.* 04 (2017) 161.
- [18] M. Hoferichter, B.-L. Hoid, B. Kubis, S. Leupold, S. Schneider, Dispersion relation for hadronic light-by-light scattering: pion pole, *J. High Energy Phys.* 10 (2018) 141.
- [19] A. Gérardin, H. Meyer, A. Nyffeler, Lattice calculation of the pion transition form factor with $N_f = 2 + 1$ Wilson quarks, *Phys. Rev. D* 100 (3) (2019) 034520.
- [20] Johan Bijnens, Nils Hermansson-Truedsson, Antonio Rodríguez-Sánchez, Short-distance constraints for the HLbL contribution to the muon anomalous magnetic moment, *Phys. Lett. B* 798 (2019) 134994.
- [21] Gilberto Colangelo, Franziska Hagelstein, Martin Hoferichter, Laetitia Laub, Peter Stoffer, Longitudinal short-distance constraints for the hadronic light-by-light contribution to $(g - 2)_\mu$ with large- N_c Regge models, *J. High Energy Phys.* 03 (2020) 101.
- [22] T. Blum, N. Christ, M. Hayakawa, T. Izubuchi, L. Jin, C. Jung, C. Lehner, Hadronic light-by-light scattering contribution to the muon anomalous magnetic moment from lattice QCD, *Phys. Rev. Lett.* 124 (13) (2020) 132002.
- [23] G. Colangelo, M. Hoferichter, M. Nyffeler, A. Passera, P. Stoffer, Remarks on higher-order hadronic corrections to the muon $g - 2$, *Phys. Lett. B* 735 (2014) 90–91.
- [24] Michel Davier, Andreas Hoecker, Bogdan Malaescu, Zhiqing Zhang, Reevaluation of the hadronic contributions to the muon $g - 2$ and to $\alpha(M_Z)$, *Eur. Phys. J. C* 71 (2011) 1515, Erratum: *Eur. Phys. J. C* 72 (2012) 1874.
- [25] Yuan Li, Exotics and BSM in ATLAS and CMS (non dark matter searches), *PoS CORFU2019* (2020) 051.
- [26] A. Bailey, Searches for BSM Higgs bosons at ATLAS and CMS, *PoS LHCP2020* (2021) 011.
- [27] Michaela Queitsch-Maitland, Dark sector searches with the ATLAS and CMS experiments, *PoS LHCP2020* (2021) 111.
- [28] Roel Aaij, et al., Measurement of the $B_s^0 \rightarrow \mu^+ \mu^-$ decay properties and search for the $B^0 \rightarrow \mu^+ \mu^-$ and $B_s^0 \rightarrow \mu^+ \mu^- \gamma$ decays, 8 2021.
- [29] N. Aghanim, et al., Planck 2018 results. VI. Cosmological parameters, *Astron. Astrophys.* 641 (2020) A6, Erratum: *Astron. Astrophys.* 652 (2021) C4.
- [30] Gianfranco Bertone, Dan Hooper, Joseph Silk, Particle dark matter: evidence, candidates and constraints, *Phys. Rep.* 405 (2005) 279–390.
- [31] Giorgio Arcadi, Maira Dutra, Pradipta Ghosh, Manfred Lindner, Yann Mambrini, Mathias Pierre, Stefano Profumo, Farinaldo S. Queiroz, The waning of the WIMP? A review of models, searches, and constraints, *Eur. Phys. J. C* 78 (3) (2018) 203.
- [32] Chih-Ting Lu, Raymundo Ramos, Yue-Lin Sming Tsai, Shedding light on dark matter with recent muon $(g - 2)$ and Higgs exotic decay measurements, 4 2021.
- [33] Talal Ahmed Chowdhury, Shaikh Saad, Non-Abelian vector dark matter and lepton $g - 2$, *J. Cosmol. Astropart. Phys.* 10 (2021) 014.
- [34] Giorgio Arcadi, Lorenzo Calibbi, Marco Fedele, Federico Mescia, Muon $g - 2$ and B -anomalies from dark matter, *Phys. Rev. Lett.* 127 (6) (2021) 061802.
- [35] Peter Athron, Csaba Balázs, Douglas H.J. Jacob, Wojciech Kotlarski, Dominik Stöckinger, Hyejung Stöckinger-Kim, New physics explanations of a_μ in light of the FNAL muon $g - 2$ measurement, *J. High Energy Phys.* 09 (2021) 080.
- [36] Giorgio Arcadi, Álvaro S. De Jesus, Têssio B. De Melo, Farinaldo S. Queiroz, Yoxara S. Villamizar, A 2HDM for the $g - 2$ and, *Dark Matter* 4 (2021).
- [37] Timothy Hapitas, Douglas Tucker, Yue Zhang, General Kinetic Mixing in Gauged $U(1)_{L_\mu - L_\tau}$ Model for Muon $g - 2$ and Dark Matter, 8 2021.
- [38] Jan Tristram Acuña, Patrick Stengel, Piero Ullio, A Minimal Dark Matter Model for Muon $g - 2$ with Scalar Lepton Partners up to the TeV Scale., 12 2021.
- [39] Giorgio Arcadi, Lorenzo Calibbi, Marco Fedele, Federico Mescia, Systematic approach to B -anomalies and t -channel dark matter, *Phys. Rev. D* 104 (11) (2021) 115012.
- [40] Lorenzo Calibbi, Robert Ziegler, Jure Zupan, Minimal models for dark matter and the muon $g - 2$ anomaly, *J. High Energy Phys.* 07 (2018) 046.
- [41] A. Djouadi, et al., Benchmark scenarios for the NMSSM, *J. High Energy Phys.* 07 (2008) 002.
- [42] Giorgio Arcadi, Abdelhak Djouadi, Martti Raidal, Dark matter through the Higgs portal, *Phys. Rep.* 842 (2020) 1–180.
- [43] S. Ipek, D. McKeen, A.E. Nelson, A renormalizable model for the galactic center gamma ray excess from dark matter annihilation, *Phys. Rev. D* 90 (5) (2014) 055021.
- [44] Dorival Gonçalves, Pedro A.N. Machado, Jose Miguel No, Simplified models for dark matter face their consistent completions, *Phys. Rev. D* 95 (5) (2017) 055027.
- [45] Martin Bauer, Ulrich Haisch, Felix Kahlhoefer, Simplified dark matter models with two Higgs doublets: I. Pseudoscalar mediators, *J. High Energy Phys.* 05 (2017) 138.
- [46] Patrick Tunney, Jose Miguel No, Malcolm Fairbairn, Probing the pseudoscalar portal to dark matter via $bbZ(\rightarrow \ell\ell) + E_T$: from the LHC to the galactic center excess, *Phys. Rev. D* 96 (9) (2017) 095020.
- [47] Tomohiro Abe, et al., LHC dark matter working group: next-generation spin-0 dark matter models, *Phys. Dark Universe* 27 (2020) 100351.
- [48] E. Aprile, et al., Dark matter search results from a one ton-year exposure of XENON1T, *Phys. Rev. Lett.* 121 (11) (2018) 111302.
- [49] Athanasios Dedes, Howard E. Haber, Can the Higgs sector contribute significantly to the muon anomalous magnetic moment?, *J. High Energy Phys.* 05 (2001) 006.
- [50] A. Djouadi, T. Kohler, M. Spira, J. Tutas, (e b), (e t) type leptoquarks at e p colliders, *Z. Phys. C* 46 (1990) 679–686.
- [51] Darwin Chang, We-Fu Chang, Chung-Hsien Chou, Wai-Yee Keung, Large two loop contributions to $g - 2$ from a generic pseudoscalar boson, *Phys. Rev. D* 63 (2001) 091301.
- [52] F. Larios, G. Tavares-Velasco, C.P. Yuan, A very light CP odd scalar in the two Higgs doublet model, *Phys. Rev. D* 64 (2001) 055004.
- [53] Victor Ilisie, New Barr-Zee contributions to $(g - 2)_\mu$ in two-Higgs-doublet models, *J. High Energy Phys.* 04 (2015) 077.
- [54] P.M. Ferreira, B.L. Gonçalves, F.R. Joaquim, Marc Sher, $(g - 2)_\mu$ in the 2HDM and slightly beyond: an updated view, *Phys. Rev. D* 104 (5) (2021) 053008.
- [55] A. Jueid, J. Kim, S. Lee, J. Song, Type-X two-Higgs-doublet model in light of the muon $g - 2$: confronting Higgs and collider data, *Phys. Rev. D* 104 (9) (2021) 095008.
- [56] Jin Chun Eung, Tanmoy Mondal, Leptophilic bosons and muon $g - 2$ at lepton colliders, *J. High Energy Phys.* 07 (2021) 044.
- [57] G.C. Branco, P.M. Ferreira, L. Lavoura, M.N. Rebelo, Marc Sher, Joao P. Silva, Theory and phenomenology of two-Higgs-doublet models, *Phys. Rep.* 516 (2012) 1–102.
- [58] Abdelhak Djouadi, The anatomy of electro-weak symmetry breaking. II. The Higgs bosons in the minimal supersymmetric model, *Phys. Rep.* 459 (2008) 1–241.
- [59] J. de Blas, M. Ciuchini, E. Franco, A. Goncalves, S. Mishima, M. Pierini, L. Reina, L. Silvestrini, Global analysis of electroweak data in the Standard Model, 12 2021.
- [60] G. Arcadi, A. Djouadi, The 2HD+a model for a combined explanation of the possible excesses in the CDF M_W measurement and $(g - 2)_\mu$ with Dark Matter, 4 2022.
- [61] T. Aaltonen, et al., High-precision measurement of the W boson mass with the CDF II detector, *Science* 376 (6589) (2022) 170–176.
- [62] J. Haller, A. Hoecker, R. Kogler, K. Mönig, T. Peiffer, J. Stelzer, Update of the global electroweak fit and constraints on 2HDMs, *Eur. Phys. J. C* 78 (8) (2018) 675.
- [63] Manfred Lindner, Moritz Platscher, Farinaldo S. Queiroz, A call for new physics: the muon anomalous magnetic moment and lepton flavor violation, *Phys. Rep.* 731 (2018) 1–82.
- [64] Shinya Kanemura, Yasuhiro Okada, Eibun Senaha, C.P. Yuan, Higgs coupling constants as a probe of new physics, *Phys. Rev. D* 70 (2004) 115002.
- [65] Giorgio Arcadi, Giorgio Busoni, Thomas Hügler, Valentin Titus Tenorth, Comparing 2HDM + scalar and pseudoscalar simplified models at LHC, *J. High Energy Phys.* 06 (2020) 098.
- [66] G. Aad, et al., Search for heavy Higgs bosons decaying into tau leptons with the ATLAS detector using pp collisions at $\sqrt{s} = 13$ TeV, *Phys. Rev. Lett.* 125 (5) (2020) 051801.
- [67] A. Djouadi, L. Maiani, G. Moreau, A. Polosa, J. Quevillon, V. Riquer, The post-Higgs MSSM scenario: habemus MSSM?, *Eur. Phys. J. C* 73 (2013) 2650.
- [68] A. Djouadi, L. Maiani, A. Polosa, J. Quevillon, V. Riquer, Fully covering the MSSM Higgs sector at the LHC, *J. High Energy Phys.* 06 (2015) 168.
- [69] Emanuele Bagnaschi, et al., MSSM Higgs boson searches at the LHC: benchmark scenarios for run 2 and beyond, *Eur. Phys. J. C* 79 (7) (2019) 617.
- [70] Georges Aad, et al., Search for charged Higgs bosons decaying into a top quark and a bottom quark at $\sqrt{s} = 13$ TeV with the ATLAS detector, *J. High Energy Phys.* 06 (2021) 145.
- [71] Spyros Argyropoulos, Ulrich Haisch, Benchmarking LHC searches for light 2HDM+a pseudoscalars, 2 2022.
- [72] Albert M. Sirunyan, et al., Search for a narrow resonance lighter than 200 GeV decaying to a pair of muons in proton-proton collisions at $\sqrt{s} = 13$ TeV, *Phys. Rev. Lett.* 124 (13) (2020) 131802.
- [73] Roel Aaij, et al., Searches for low-mass dimuon resonances, *J. High Energy Phys.* 10 (2020) 156.
- [74] Michael Spira, HIGLU: a program for the calculation of the total Higgs production cross-section at hadron colliders via gluon fusion including QCD corrections, 10 1995.
- [75] A. Djouadi, J. Kalinowski, M. Spira, HDECAY: a program for Higgs boson decays in the standard model and its supersymmetric extension, *Comput. Phys. Commun.* 108 (1998) 56–74.
- [76] Abdelhak Djouadi, Jan Kalinowski, Margarete Muehlleitner, Michael Spira, HDECAY: twenty++ years after, *Comput. Phys. Commun.* 238 (2019) 214–231.
- [77] Tomohiro Abe, et al., LHC dark matter working group: next-generation spin-0 dark matter models, *Phys. Dark Universe* 27 (2020) 100351.
- [78] Constraints on mediator-based dark matter models using $\sqrt{s} = 13$ TeV pp collisions at the LHC with the ATLAS detector, 11 2018.
- [79] Luigi Delle Rose, Shaaban Khalil, Stefano Moretti, The muon $g - 2$ in an Aligned 2-Higgs Doublet Model with Right-Handed Neutrinos, 11 2021.
- [80] A. Djouadi, P.M. Zerwas, J. Zunft, Search for light pseudoscalar Higgs bosons in Z decays, *Phys. Lett. B* 259 (1991) 175–181.

- [81] R. Barate, et al., Search for the standard model Higgs boson at LEP, *Phys. Lett. B* 565 (2003) 61–75.
- [82] Ulrich Haisch, Jernej F. Kamenik, Augustinas Malinauskas, Michael Spira, Collider constraints on light pseudoscalars, *J. High Energy Phys.* 03 (2018) 178.
- [83] Combination of searches for invisible Higgs boson decays with the ATLAS experiment, 10 2020.
- [84] Tomohiro Abe, Ryosuke Sato, Kei Yagyu, Lepton-specific two Higgs doublet model as a solution of muon $g - 2$ anomaly, *J. High Energy Phys.* 07 (2015) 064.
- [85] S. Heinemeyer, W. Hollik, The decay $h_0 \rightarrow A_0 A_0$: a complete one loop calculation in the MSSM, *Nucl. Phys. B* 474 (1996) 32–56.
- [86] Adam Alloul, Neil D. Christensen, Céline Degrande, Claude Duhr, Benjamin Fuks, FeynRules 2.0 - a complete toolbox for tree-level phenomenology, *Comput. Phys. Commun.* 185 (2014) 2250–2300.
- [87] G. Passarino, M.J.G. Veltman, One loop corrections for $e^+ e^-$ annihilation into $\mu^+ \mu^-$ in the Weinberg model, *Nucl. Phys. B* 160 (1979) 151–207.
- [88] Vladyslav Shtabovenko, FeynHelpers: connecting FeynCalc to FIRE and package-X, *Comput. Phys. Commun.* 218 (2017) 48–65.
- [89] Matthew J. Dolan, Felix Kahlhoefer, Christopher McCabe, Kai Schmidt-Hoberg, A taste of dark matter: flavour constraints on pseudoscalar mediators, *J. High Energy Phys.* 03 (2015) 171, Erratum: *J. High Energy Phys.* 07 (2015) 103.
- [90] Giorgio Arcadi, Manfred Lindner, Farinaldo Queiroz, Werner Rodejohann, Stefan Vogl, Pseudoscalar mediators: a WIMP model at neutrino floor, *J. Cosmol. Astropart. Phys.* 03 (2018) 042.
- [91] J.P. Lees, et al., Search for a dark leptophilic scalar in e^+e^- collisions, *Phys. Rev. Lett.* 125 (18) (2020) 181801.
- [92] Eung Jin Chun, Jinsu Kim, Leptonic precision test of leptophilic two-Higgs-doublet model, *J. High Energy Phys.* 07 (2016) 110.
- [93] Mikolaj Misiak, Matthias Steinhauser, Weak radiative decays of the B meson and bounds on M_{H^\pm} in the two-Higgs-doublet model, *Eur. Phys. J. C* 77 (3) (2017) 201.
- [94] Tomohiro Abe, Motoko Fujiwara, Junji Hisano, Loop corrections to dark matter direct detection in a pseudoscalar mediator dark matter model, *J. High Energy Phys.* 02 (2019) 028.
- [95] Fatih Ertas, Felix Kahlhoefer, Loop-induced direct detection signatures from CP-violating scalar mediators, *J. High Energy Phys.* 06 (2019) 052.
- [96] Nicole F. Bell, Giorgio Busoni, Isaac W. Sanderson, Loop effects in direct detection, *J. Cosmol. Astropart. Phys.* 08 (2018) 017, Erratum: *J. Cosmol. Astropart. Phys.* 01 (2019) E01.
- [97] M. Ackermann, et al., Searching for dark matter annihilation from milky way dwarf spheroidal galaxies with six years of Fermi large area telescope data, *Phys. Rev. Lett.* 115 (23) (2015) 231301.
- [98] M. Ackermann, et al., Updated search for spectral lines from galactic dark matter interactions with pass 8 data from the Fermi LAT, *Phys. Rev. D* 91 (12) (2015) 122002.
- [99] Stephen M. Barr, A. Zee, Electric dipole moment of the electron and of the neutron, *Phys. Rev. Lett.* 65 (1990) 21–24, Erratum: *Phys. Rev. Lett.* 65 (1990) 2920.
- [100] Robert V. Harlander, Stefan Liebler, Hendrik Mantler, SusHi: a program for the calculation of Higgs production in gluon fusion and bottom-quark annihilation in the Standard Model and the MSSM, *Comput. Phys. Commun.* 184 (2013) 1605–1617.